Ecology Monitoring in Forests with Aerial Robots

Salua Hamaza, André Farinha, Hai-Nguyen Nguyen and Mirko Kovac

***Abstract*— Research into remote sensing tools for environmental monitoring is an essential aspect for ensuring a healthy an thriving biosphere under the canopy, but also for preventing forest-related hazards from occurring. The challenges associated with forestry robotics are posed by the environment itself, as forests are wide-spread areas with a high density of obstacles and complex geometries to navigate in. Multirotors are Unmanned Aerial Vehicles (UAVs) that offer great agility and an unbounded operational workspace within a compact size. These features make their deployment in such wide areas most suitable for depositing wireless sensor networks that provide real-time forest monitoring. Hence, within this paper we propose a novel paradigm to ecology monitoring which exploits UAVs as the carriers of environmental sensors to be deployed in forests. Three different methodologies and systems are hereby presented and discussed for sensor placement tasks, leveraging bespoke design, navigation and control techniques.**

I. INTRODUCTION

UAVs have been used effectively for data acquisition in forested environments [1]–[3]. This generates spatially dense, yet sparse time series, often not ideal for ecological studies that monitor long-term changes on the environment. Hence the need to perform frequent flights, which increases the costs and manpower needed for such studies. Having the capability to deploy sensors from UAVs can significantly reduce the effort of acquiring datasets with appropriate spatial and temporal resolution, as the deployed sensors can complement spatially dense UAV data with temporally dense data. Moreover, the measurement of environmental variables along the strata of a forest, which is a lengthy and hazardous exploit, can be simplified by UAV sensor placement. This requires, however, the usage of multiple solutions, given the inherently different topology found in forest strata. The understorey layer is often (but not always), clear of brush and other obstacles, creating direct access to tree trunks where sensors can be securely attached. The canopy layer is very cluttered with branches and foliage, which is hazardous for flight. However, vertical corridors can often be found where UAVs can operate as long as a safety distance is kept from obstacles. The emergent layer is mostly unobstructed, creating ideal conditions for flight, and punctuated by larger trees that emerge above the canopy. These trees are also viable targets for sensor deployment.

Within this paper we propose three different strategies for tackling environmental monitoring in forests using multirotors, as illustrated in Figure 1. Each proposed solution entails a combination of bespoke mechanism designs and control approaches to address sensor delivery on trees. The first strategy consists in the proposition of direct placement of sensors on tree trunks using vision-based perception and autonomous navigation. The second method consists of using the multirotor itself as a mobile sensing device by exploiting the ability to perch on tree branches. Perching is herein presented as a way to overcome the poor endurance of flying robots, by adopting idle state while sensory data are collected passively in the emergent layer of the canopy. The third strategy brings a novel methodology to sensor deployment via impulsive launch, offering a good trade-off for deploying sensors in the more cluttered stratum of the canopy.

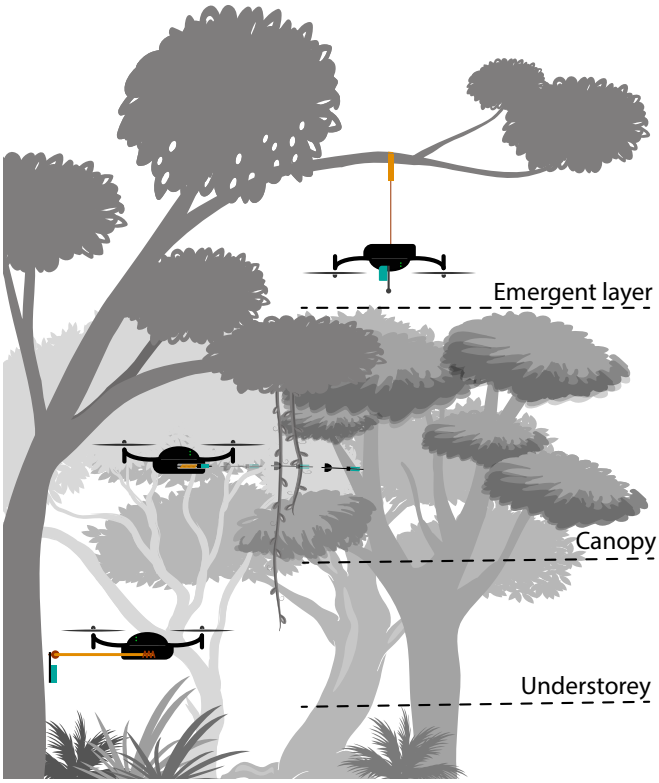

Fig. 1: Illustration showing the 3 delivery methods proposed.

Extensive experiments have been conducted for each of these strategies, which have also proved robust and reliable in the outdoor setting.

II. ENVIRONMENTAL SENSORS DELIVERY METHODS

When using UAVs to deliver sensors in the environment, two approaches can be followed: *direct* and *indirect*. In the direct approach, contact is established between the flying robot and the target environment. The state-of-the-art in aerial robotic

All authors are with the Aerial Robotics Laboratory, Imperial College London, South Kensington, United Kingdom. Mirko Kovac is also with the Swiss Federal Laboratories for Materials Science and Technology (EMPA), Ueberlandstrasse 129, 8600 Dubendorf, Switzerland.
E-mail addresses: s. hamaza; a.farinha17; h.nguyen; m.kovac@imperial.ac.uk

manipulation offers various examples where UAVs are equipped with active manipulators for contact-based interaction [4]. Several challenges are faced when establishing direct contact between the aircraft and the target, such as flight instability due to the induced angular momentum [5], a higher risk of failure due to the close proximity with the target, the ability to deliver a smooth and compliant interaction by monitoring the force exchange [6]–[9]. For these reasons, the direct method is most suited in scenarios where a high positioning accuracy and a controlled force exchange are required for the interaction.

The indirect method entails the deployment of sensors without the need for contact, by either dropping from height or launching from a distance. Such method can be advantageous in those instances where the target surface is not easily accessible, or the exchange force and positioning accuracy are not a major concern.

Aerial sensor dropping techniques often involve the use of a sensor pod with control surfaces that allow to adjust the sensor trajectory prior to fall. Examples of this can be seen in [10]–[12]. Aerial drop represents an intuitive and effective solution to sensor deployment, which also retains high robustness for field operation thanks to the limited onboard computation and limited automation required.

Impulsive sensor deployment (or launching) can achieve a good compromise between positioning accuracy and clearance from obstacles. To the best of our knowledge, this type of indirect method has not been studied thus far in the literature.

TABLE I: Comparison of sensor delivery methods found in the literature and our proposed strategies.

	Direct[13,14,*]	Drop[12]	Perch[18,19]	Launch*
accuracy	±0.025 m	±4 m	±0.5 m	±0.1 m
safety distance	0 m	>10 m	<10 m	4 m
total mass	<2.4 kg	<2 kg†	<1.7 kg	0.65 kg
sensor number	single	multiple	multiple	single

Looking at Table I, it can be noted that direct sensor placement solutions offer a higher positioning accuracy with respect to indirect methods, at the expense of higher complexity in the control and navigation techniques. On the other hand, indirect methods offer scalable sensor deployment with greater clearance from obstacles and with lower risks.

Within the next sections, three different approaches to environmental monitoring using multirotors are presented and discussed, using both direct and indirect strategies.

III. DIRECT SENSOR PLACEMENT

Direct sensor placement using multirotors is a new area of interest within the aerial robotics community. Thus far, only two works have addressed this type of task and tailored it for sensor deployment on a wall or tree [13], [14]. The former work highlights the use of an off-the-shelf quick-release mechanism embedded on a customised aerial platform. To deliver the force at the tool-tip, the authors make use of a horizontally-mounted propeller which conveys a force normal to a vertical wall via a passive tool. The latter work integrates an active 1-degree-of-freedom manipulator onboard the UAV, capable of generating a force normal to the wall by means of a motorised rack-and-pinion transmission. Such force output is combined with the pitching action of the underactuacted quadrotor to provide higher force values at the end-effector. The approach is successfully tested indoors and outdoors against tree trunks.

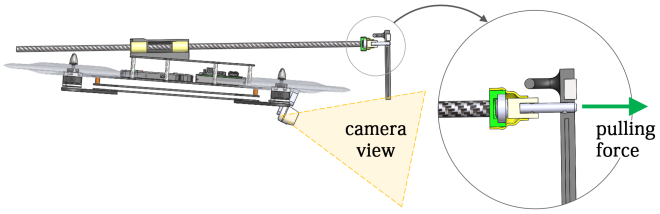

Fig. 2: Passively compliant mechanism for direct sensor placement.

Within this section we aim to introduce our approach on autonomous sensor placement performed by a quadrotor equipped with a compact and lightweight mechanism. The contribution is the proposition of a new architecture that combines mechanical compliance, control and path planning to achieve autonomous placement of sensors within the environment. The strategy hereby proposed is tailored for off-the-shelf quadrotors and accounts for their intrinsic limitations in terms of actuation (maximum thrust vector) and underactuation constraints (coupling between rotational and translational dynamics). This approach particularly focuses on exploiting the platform's capabilities in terms of force generation and path planning, without the use of redundant sensing or actuation. Along the same lines, the mechanism design for delivering the sensor is simple and lightweight as this approach aims to stress on control robustness to achieve precise and repeatable outcome.

A. Mechanism Design

The mechanism is a passive 1-degree-of-freedom tool consisting of a carbon fibre tubular rod that can slide inside two linear bearings, housed in a 3D printed case. Compliance is integrated in the design both at the tool tip and in the 3D printed housing by means of rubber membranes that smooth the motion of the slider.

The tool tip is designed to act as a quick-release mechanism. A spherical bushing holds a quick-release pin in place while a rubber membrane allows for small angular corrections during placement, adding compliance. The quick-release pin has one end fixed with the spherical bushing, while the free end is press fitted inside the sensor case, as illustrated in Fig. 2. When a force causes the sensor to be pulled away, the pin slides out of the sensor, facilitated by a spring-loaded ball on the pin itself. To adhere the sensor on the target surface, a Neodymium magnet is slotted inside the sensor case. Such magnet provides the pulling force required to release the sensor from the tool tip when in contact with a metal surface.

B. Vision-based Perception

Visual odometry is computed on-board to perceive and navigate the quadcopter autonomously towards the target. Two Intel® stereo cameras are mounted at the front of the vehicle for depth sensing and visual odometry, RealSense D435 and T265 respectively.

In order to determine the target surface, a 3D collection of points in space (point cloud) is used as the input. The normal

* Based on the work shown in this paper.
†Estimated value.

Fig. 3: Direct sensor placement on a tree with an aerial robot.

vector originating from the centre of a planar surface is computed from the sensed input using the RANSAC method, due to its robustness and simplicity. Normals to the target surface are found by calculating a plane tangent to the target surface, which becomes a least-square plane fitting estimation problem. An average normal bearing is determined as the mean of all computed normals, with a target location defined as the mean of all computed normal positions. When the bearing of the output normal vector is determined to be within a defined threshold, the vehicle recognises that a vertical surface is within the field of view of the sensor. The origin of such a vector is then set as the target sensor placement location and a trajectory is generated.

C. Motion Control

The coupling between the attitude and the translational dynamics of the quadrotor makes direct control of the tool-tip position challenging, requiring more complex low-level attitude control, previously published in [15]. Here we present a high-level attitude controller (thrust vector) to accomplish point-to-point motion with the aim of reducing the complexity and increasing the robustness.

To control the quadrotor translational dynamics, the thrust vector $\Lambda := \lambda R e_3 \in \Re^3$ is used as the control input. The PD control of the translation dynamic can be derived as follows

$$\Lambda = mge_3 + m\ddot{x}_d - k_b(\dot{x} - \dot{x}_d) - k_p(x - x_d) \tag{1}$$

with $x_d(t) \in \Re^3$ being the desired trajectory. Note here that, without disturbances and uncertainty, the errors will exponentially converge to zero.

The thrust control is then decoded into the desired thrust, roll, pitch, yaw command for the low-level attitude controller. Following [8], the thrust command can be computed directly as $\lambda = \|\Lambda\|$. To compute yaw, pitch, roll angles $[\phi;\theta;\psi] \in \Re^3$, we use the parameterized rotation matrix $R = R_{e_3}(\phi)R_{e_2}(\theta)R_e(\psi)$ with $R_e(\star)$ being the elementary rotation matrix about the e_i-axis. The yaw angle ϕ_i can be chosen arbitrarily. For example, we can choose yaw command to ensure that the tool is always perpendicular to the target surface. The roll and pitch command can be determined using the following relation

$$R_{e_2}(\theta)R_{e_1}(\psi)e_3 = \begin{bmatrix} \sin\theta\cos\psi \\ -\sin\psi \\ \cos\theta\cos\psi \end{bmatrix} = \hat{\Lambda}(\phi)$$

with $\hat{\Lambda}(\phi) := \frac{1}{\lambda} R^T_{e_3}(\phi)\Lambda$. We then can choose the roll and pitch commands as

$$\psi_d = -\sin^{-1}\hat{\Lambda}_2, \qquad \theta_d = \tan^{-1}\frac{\hat{\Lambda}_1}{\hat{\Lambda}_3},$$

with $\hat{\Lambda}_i$ being the ith element of $\hat{\Lambda}$.

For given desired trajectory $x_d(t)$, we now can compute the desired attitude R_d. The attitude commands is then sent to the lower-level controller in the flight control unit for trajectory tracking.

D. Interaction Control

To address the physical interaction between the aerial robot and the environment, we make use of an admittance controller. Such approach will focus on the interaction force generated at the tool only, discarding external disturbances such as the wind effect [16]. Moreover, it is assumed that the interaction is of type *point-contact*. Hence, the virtual dynamic system can be written as:

$$m_d\ddot{e}_r + b_d\dot{e}_r + k_d e_r = f_e \tag{2}$$

where $e_r := x_d - x_r$ with $x_r(t) \in \Re^3$ being the generated reference trajectory, m_d,b_d,k_d are the desired virtual inertia, damping and spring. Note here that the translation and rotation on the quadrotor are coupling. We can shape the interaction of the quadrotor either on the translation or rotation layer. In this work, we choose the translation layer and observe that it is adequate to add necessary compliant element to the inner PID control loop.

Several calibration experiments were conducted where the quadrotor was purposely disturbed with an unknown external force by manually pulling it with a rope. It was observed that for low-stiff parameters, e.g., $k_d = 5$, the vehicle follows the cable force closely and for critical damping, $m_d = 1$,$b_d = 10$,$k_d = 25$ the steady-state returns back to the desired motion quickly when the cable is released. This showed that the interactive behaviour could be shaped accordingly to the target's stiffness.

E. Experiments

The platform used for the implementation is the quadrotor Lumenier QAV400, with flight controller unit (FCU) Pixhawk® Pixracer. The onboard computer used for path planning and force estimation is the Intel® UP CORE board.

In figure 4, the drone's pose and force are illustrated during experiments. Moving forward in the x-direction, the vehicle follows the generated trajectory towards the target location. At $t = 12$ seconds, the vehicle makes contact with the target surface. This is also reflected in the interaction force plot at the bottom of the figure The overall contact phase can be seen in the x-direction, from $t = 12$ to $t = 16$ seconds. Contact is considered *established* when the force in the direction of travel has reached a predefined threshold, after which the robot retreats from surface, leaving the sensor in the desired location (from $t = 16$ to $t = 18$ seconds). It can be clearly seen that the interaction force in the direction of travel during this phase is large relative to the contact phase force. Such a phenomenon is due to the mechanism holding the sensor which requires a substantial pulling force in order to release the sensor in place. This behaviour is desired as it guarantees robustness and avoids the sensor from falling in free flight. The required force can however be adjusted to any desired value by using a lower friction release mechanism.

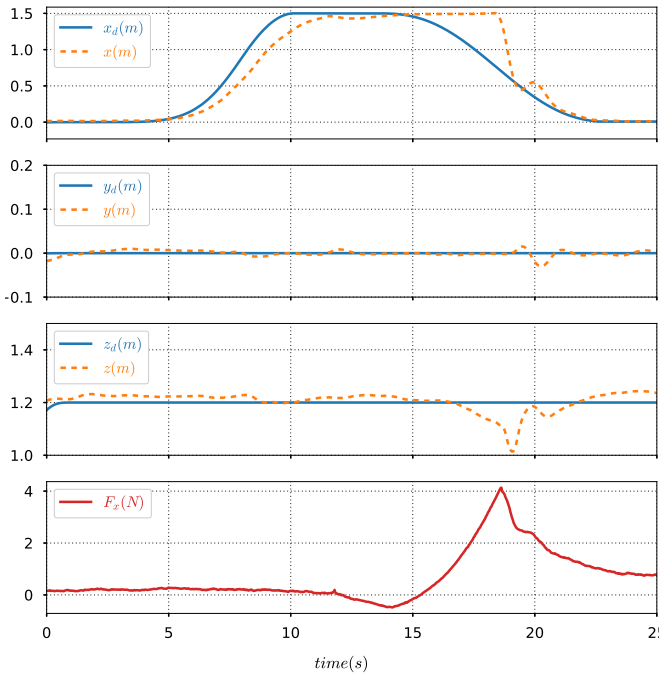

Fig. 4: Position tracking and acceleration-based force estimation for sensor placement task. The target surface is on the x-axis of the robot.

Fig. 5: Sequence of tensile perching performed on a tree.

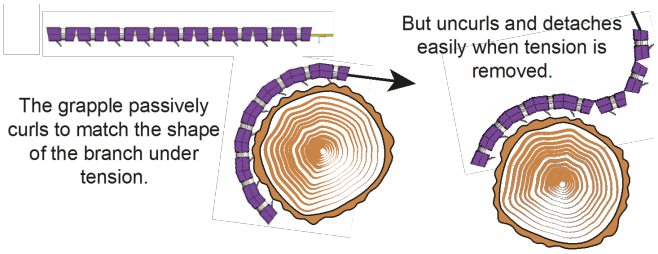

Fig. 6: The compliant grapple passively curls to the shape of the branch, engaging the microspines to distribute the load, while still being easily detachable.

IV. PERCHING ON TREES & SENSOR DROPPING

Mimicking the behaviour of birds flocking above the canopy, multirotors can land on tree branches and observe the environment while remaining idle [17], [18]. With the ability to perch, a flying vehicle would be able to safely gather forest data while preserving battery life and retaining manoeuvrability. Such approach to environmental monitoring offers the flexibility of using the UAV as a *mobile sensing device*, but not only. In fact, such flying robot could also act as a temporary gateway for communication networks in remote areas, or facilitate aerial sensor dropping by shortening the drop height for a softer and safer fall.

Within this section, we present a passively adaptive perching mechanism which allows an aerial vehicle to stably attach to a tree branch, together with motion control techniques used to achieve this result.

A. Adaptive Microspine Grapple

Perching on a tree branch is enabled by a compliant grapple module, which passively conforms to the surface of convex perching targets, ensuring reliable traction and a reliable load capacity (of above 60 kg in some instances) whilst still releasing effortlessly.

The grapple is formed from individual plastic links with a trapezoidal cross section, see Figure 6 . Each link slides freely along a flat cable through its centre, with the exception of the final, furthest link, to which the cable is attached. The faces of each segment are angled such that when a shear force is applied to a segment, the cable tension causes the grapple to curl. Since the grapple curls only in one direction, grapples are used in pairs, attached at the first link with a common tether, such that attachment is possible from any direction. For attachment to trees, each link has a pair of sharpened steel spines protruding from the underside that ensure attachment to rough or soft surfaces.

B. Perching Control

The aerial robot uses a tether and a microspine grapple to attach to branches, by flying over the top of a perching target. The robot can detect the attachment/detachment of the grapple by estimating the interaction force using onboard IMU and additional odometry information (such as motion capture system or a VIO camera such as Intel T265). In the tethered flight mode, the robot dynamics is decomposed into constrained motion and the free motion.. . The interaction can be regulated using force feedback control, and the free .... By flying below the branch on the tether the robot can power down and conserve energy

C. Experiments

The grapple was integrated with a small multirotor of total mass 1.76 kg and a motorised winch system to allow movement on the perch. The perching sequence was tested on a variety of substrates, including tree branches. Once the robot attaches to the

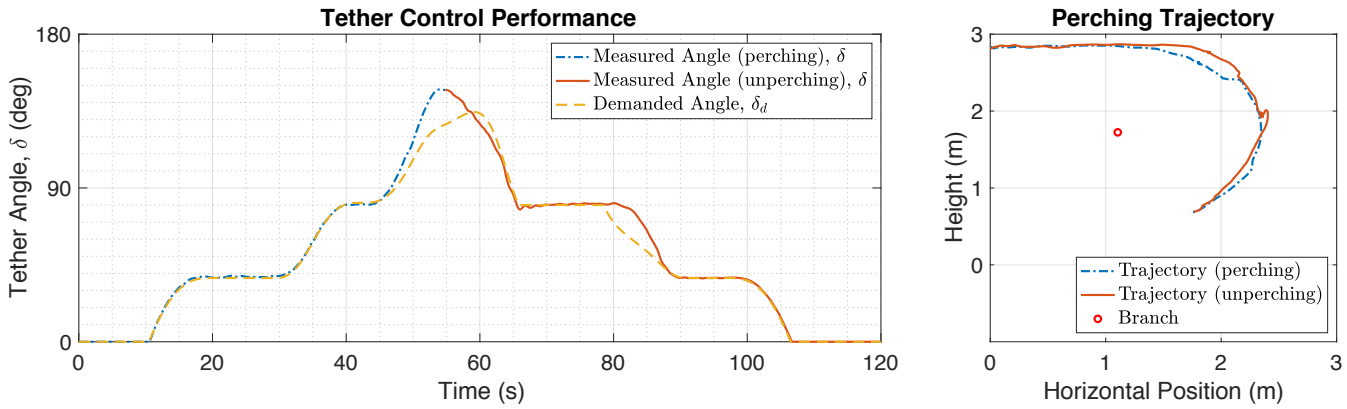

Fig. 7: Tensile perching experiment: motion tracking of the tether angle and the UAV's center-of-mass.

branch, the flight controller can hold the UAV at any orientation, by using the grapple as a tether.

Experiments were also repeated using a magnetic grapple configuration. In this configuration, the grapple tension was less significant, however perching was reliable provided a rubber coating was used to prevent the magnets from fracturing. The performance of the controller was measured by comparing demanded angle with motion capture data during a *perch and unperch* manoeuvre, as illustrated in Figure 7. The controller was found to conform accurately to the position demands, and to respond effectively when the command angle was changed as the perch sequence progressed.

V. SENSOR LAUNCHING

In certain scenarios, there is a need to deploy sensors in cluttered environments e.g. the forest canopy. While dropping a sensor from above the canopy is a viable solution, this does not allow for a sensor to be deployed accurately and securely on a tree branch. There is thus a need for some compromise between clearance from obstacles in the canopy and accuracy. Impulsive sensor deployment (or launching) achieves such a compromise, by maintaining a distance from tree branch, where foliage and other branches can be located. UAV based sensor placement accuracy, and in certain cases success, is limited by the UAV state and position estimation, as well as error in the target position estimation. However, in this case, there is the added factor of uncertainty in the trajectory of the sensor during launch. On the other hand, such a system can be designed to be very lightweight and compact. Something advantageous when flying through cluttered environments.

A. Launching Mechanism Design

The design of an impulsive launching system should allow operations in cluttered environments and the deployment of sensors within a radius smaller that the smallest feature where a measurement is necessary. This can be for example a 20 cm tree branch. The task should be achieved with a clearance of up to 3 m from the target to keep the aircraft further away from potential obstacles in the environment. Furthermore, the mass of the system should remain below 1 kg to keep the UAV as small and nimble as possible. As for the sensor to be launched, 30 g is enough to accommodate a small IOT sensor and peripherals. The design strategy for such a system is centred on its energy flow, as the amount and nature of the energy stored is directly linked to the sizing of the system. Starting by defining the amount of energy necessary to attach the sensor to the wood, or bark, of a certain tree, one can work it's way backwards estimating the amount of energy dissipated in projectile motion and losses in energy conversion. With this information, the energy storage mode can be chosen, followed by the trigger that releases this energy and finally the multicopter platform can be sized.

Penetrating spines have been shown to be a good option to perch UAVs in forests [19], hence their use is appropriate to attach sensors on trees. This requires, however, a considerable amount of energy which is dissipated through plastic deformation and friction. The required energy can be estimated using data from [20] and integrating the indentation energy of a conical indenter [21]. One can further assume that the spines will actually attach to the bark layer. It has been shown that oak's bark shear strength is approximately 12% that of its wood [22] and this ratio is adopted throughout. A list of common woods and bark are shown in Table II.

TABLE II: Estimated indentation energy for different types of wood.

	Red Pine	Birch	Chestnut	Oak	Willow
Wood	7.25 J	8.76 J	8.31 J	12.68 J	7.10 J
Bark	0.87 J	1.05 J	1.00 J	1.53 J	0.85 J

The flight of the projectile can be studied as a planar trajectory under the effect of weight and drag. The resulting equations of motion can be solved as an initial value problem, however, one of the boundary conditions is the kinetic energy at impact. Since the relation between initial and final velocity is monotonic, simple convex optimisation can be used to obtain the initial value. Taking a payload of 15-30 grams, a sphere of 25 mm diameter and drag coefficients ranging from 0.5 to 1.5 ($Re \sim 10^4$) one obtains that the kinetic energy at launch must be in the order of 0.94 J to 1.74 J for the considered wood barks and a 3 meter flight. Other relevant effects are, for example, the pitch yaw and roll stability of the projectile. Stability can be improved with appropriately sized fin stabilisers.

There are several means to store the energy necessary to launch a sensor. Propellant based systems are energy dense but are substantially complex limiting the ability for in field repairs. Similarly, pneumatic systems such as compressed gas launchers, need heavy high pressure gas-sealing components. For deployment on a compact and lightweight UAV, where payload weight severely limits flight endurance, mechanical launch is

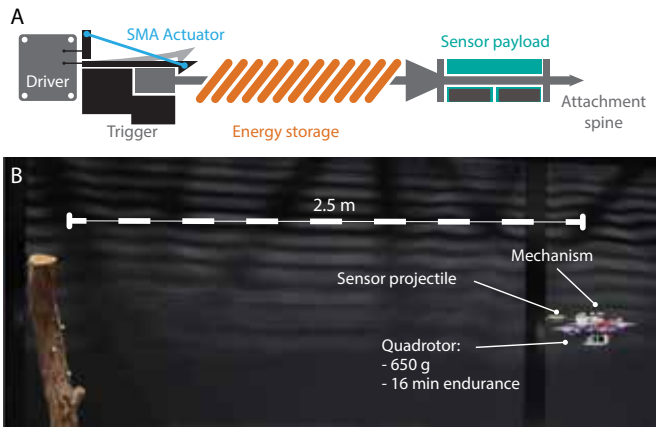

Fig. 8: Sensor launching mechanism design. **A** Illustration of the different components that make up the sensor launching system. **B** Platform used in the implementation and experimental setup for launching towards a wooden branch.

deemed to be the best solution.

All that remains is the design of an actuator that can trigger the release of the stored mechanical energy. The actuator used relies on a shape memory alloy wire which is tensioned by 2 cantilever beams. A schematic of the full system is shown in Fig. 8 and consists of a trigger mechanism with the necessary drivers for the SMA, a linear spring for energy storage, a sensor pod that includes the sear catch and a single spine for attachment. In order to avoid loss of kinetic energy in components attached to the spring or in shock absorbers, the compression of the linear spring is done using the sensor housing and the trigger mechanism hooks into a nock at the back of the sensor.

B. Experiments

A custom built platform weighing a total of 0.65 kg and with an endurance of 16 minutes is used for the implementation. The quadrotor flies autonomously, and computation of the vehicle's state is done off-board. Position commands are generated by a PID, converted to PPM and sent to the vehicle via an RC controller. Position way-points were autonomously generated to guide the quadrotor to the best launch position relative to a target detected by the motion capture system. The launch position was calculated neglecting drag or other dynamic behaviours of the sensor. Once the position is reached, the launch command is sent to the flight controller (Omnibus F4 pro running the *Betaflight* firmware).

Even though possible, modelling the exact dynamics of a sensor projectile is a fruitless pursuit. In fact, a full aerodynamics characterisation is a lengthy process unlikely to be repeated for multiple sensor payloads, which would compromise the system's versatility. There is thus, the need for some compromise when predicting the trajectory of the sensor, so that generality is maintained without compromising accuracy and precision. The simplest approach was taken here: point mass ballistics, for which there is a closed for solution for the position the multirotor should take to hit the desired target.

In order to assess the performance of such a simple approximation, a total of 81 successful sensor placements were executed in laboratory conditions. Sensors were launched at

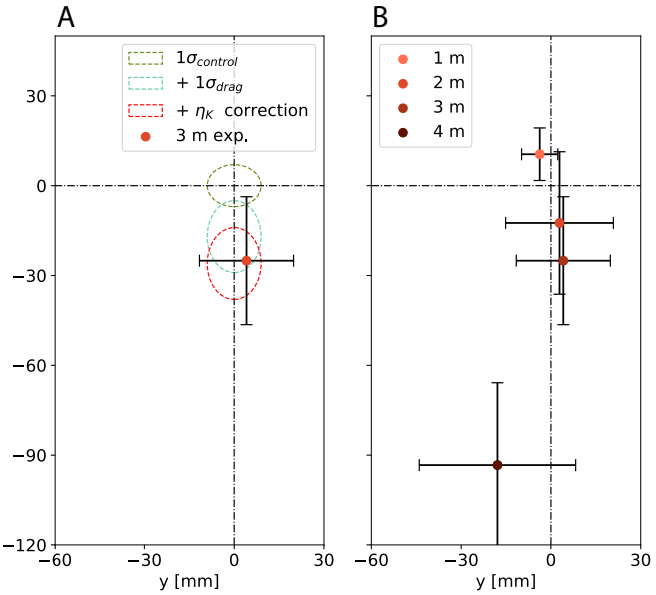

Fig. 9: Sensor placement results for the 64 tests executed on a flat metallic surface. **A:** Effect of control loop, sensor projectile drag and losses in potential - kinetic energy conversion. **B:** Mean and standard deviation of sensor placement experiments at 1 to 4 meters distance from a flat metallic surface

3 different targets: a ferromagnetic surface, a pipe of 30 cm diameter and a tree branch of 13 cm width. A magnet was used for attachment to metallic targets, and a spine for the wooden target.

Figure 9 summarises 64 indoor sensor launching experiments onto a flat metal plate target. Figure 9A shows the 1σ interval for launched from 3 meters distance. It is shown how while the scatter is a consequence of the control loop uncertainty, the vertical bias is partially caused by the fact that drag is neglected. There is yet another contribution to the bias, which is the fact that the launch speed is not as high as predicted. In fact, the estimated kinetic energy of the sensor at launch can be calculated as $K = U(1+m_s/m_{quad})$, where m_s and m_{quad} are the masses of the sensor and quadrotor, respectively. However, analysis of high speed footage shows other dissipating dynamic effects which account for a considerable amount of the vertical bias. Figure 9B shows a considerable increase in scatter and bias with distance from target. The addition of stabilising fins and the correction for energy dissipation yields improvements in both areas allowing the precise and robust targeting of 10 cm diameter branches at 3 meters distance, as shown in the sequence in Fig. 10.

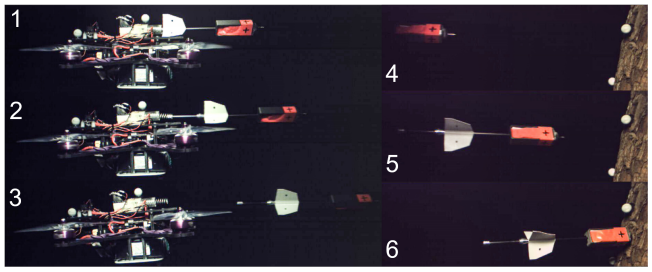

Fig. 10: Launching and impact sequence recorded at 1600 fps.

VI. CONCLUSIONS

In this paper we present three different methods for environmental monitoring using UAVs. These methods propose a novel paradigm to ecology monitoring using multirotors, where instead of on-site intervention, the aircraft is the carrier of sensor networks to be deployed in the forest. Such approach effectively enables long-term data acquisition while overcoming UAVs reduced flight time during mission. The systems proposed offer great versatility, as they can operate over a range of different forest strata and carry/deploy a range of different sensory payloads.

Within each of the three methods, we have described novel designs tailored for aerial interaction with trees, together with bespoke motion and control strategies. All systems have been robustly demonstrated outdoors on real trees, showing successful results in the field. Some challenges are however still to be addressed to fully make these systems field-ready. Among those, further developments on perception for navigation in extremely complex environments and tree interaction will be addressed in the future.

Overall the methodologies discussed in this paper represent viable solutions for forestry robotics, and a step forward in the direction of long-term ecology monitoring using wireless sensor networks.

ACKNOWLEDGMENT

The authors would like to thank Guy Burroughes for his helpful comments and interesting discussions concerning nuclear applications. The authors would also like to acknowledge the support of all collaborators at the Aerial Robotics Laboratory involved in the works promoted in this paper.

The research on *Sensor Launching* was funded by NERC/NPIF (award no. NE/R012229/1) and carried out within the framework of the EUROfusion Consortium. It has received funding from the Euratom research and training programme 2014-2018 and 2019-2020 under grant agreement No 633053. The views and opinions expressed herein do not necessarily reflect those of the European Commission. The research on *Direct Sensor Placement* and *Aerial Perching* was supported by EPSRC (awards no. EP/N018494/1, EP/R026173/1, EP/R009953/1 and EP/R02572X/1). The work of Mirko Kovac was supported by the Royal Society Wolfson fellowship (RSWF/R1/18003).

REFERENCES

[1] J. Paneque-Gálvez, M. K. McCall, B. M. Napoletano, S. A. Wich, and L. P. Koh, "Small drones for community-based forest monitoring: An assessment of their feasibility and potential in tropical areas," *Forests*, vol. 5, no. 6, pp. 1481–1507, 2014.

[2] H. T. Berie and I. Burud, "Application of unmanned aerial vehicles in earth resources monitoring: focus on evaluating potentials for forest monitoring in ethiopia," *European journal of remote sensing*, vol. 51, no. 1, pp. 326–335, 2018.

[3] M. B. Bagaram, D. Giuliarelli, G. Chirici, F. Giannetti, and A. Barbati, "Uav remote sensing for biodiversity monitoring: are forest canopy gaps good covariates?" *Remote Sensing*, vol. 10, no. 9, p. 1397, 2018.

[4] F. Ruggiero, V. Lippiello, and A. Ollero, "Aerial manipulation: A literature review," *IEEE Robotics and Automation Letters*, vol. 3, no. 3, pp. 1957–1964, 2018.

[5] P. E. I. Pounds, D. R. Bersak, and A. M. Dollar, "Stability of small-scale uav helicopters and quadrotors with added payload mass under pid control," *Auton. Robots*, vol. 33, pp. 129–142, 2012.

[6] H. W. Wopereis, J. Hoekstra, T. Post, G. A. Folkertsma, S. Stramigioli, and M. Fumagalli, "Application of substantial and sustained force to vertical surfaces using a quadrotor," in *2017 IEEE International Conference on Robotics and Automation (ICRA)*. IEEE, 2017, pp. 2704–2709.

[7] S. Hamaza, I. Georgilas, and T. Richardson, "2d contour following with an unmanned aerial manipulator: Towards tactile-based aerial navigation," in *2019 IEEE/RSJ International Conference on Intelligent Robots and Systems, IROS 2019*. IEEE, 2019, pp. 3664–3669.

[8] H. Nguyen, S. Park, J. Park, and D. Lee, "A novel robotic platform for aerial manipulation using quadrotors as rotating thrust generators," *IEEE Transactions on Robotics*, vol. 34, no. 2, pp. 353–369, 2018.

[9] M. Ryll, G. Muscio, F. Pierri, E. Cataldi, G. Antonelli, F. Caccavale, D. Bicego, and A. Franchi, "6d interaction control with aerial robots: The flying end-effector paradigm," *The International Journal of Robotics Research*, vol. 38, no. 9, pp. 1045–1062, 2019.

[10] P. Pounds and S. Singh, "Samara: Biologically inspired self-deploying sensor networks," *IEEE Potentials*, vol. 34, no. 2, pp. 10–14, 2015.

[11] S. H. Mathisen, V. Grindheim, and T. A. Johansen, "Approach methods for autonomous precision aerial drop from a small unmanned aerial vehicle," *IFAC-PapersOnLine*, vol. 50, no. 1, pp. 3566–3573, 2017.

[12] S. G. Mathisen, F. S. Leira, H. H. Helgesen, K. Gryte, and T. A. Johansen, "Autonomous ballistic airdrop of objects from a small fixed-wing unmanned aerial vehicle," *Autonomous Robots*, pp. 1–17, 2020.

[13] D. R. McArthur, A. B. Chowdhury, and D. J. Cappelleri, "Design of the interacting-boomcopter unmanned aerial vehicle for remote sensor mounting," *Journal of Mechanisms and Robotics*, vol. 10, no. 2, p. 025001, 2018.

[14] S. Hamaza, I. Georgilas, M. J. Fernandez, P. J. Sanchez-Cuevas, T. Richardson, G. Heredia, and A. Ollero, "Sensor installation and retrieval operations using an unmanned aerial manipulator," *IEEE Robotics and Automation Letters*, vol. 4, no. 3, pp. 2793 – 2800, 2019.

[15] H. Nguyen, C. Ha, and D. J. Lee, "Mechanics, control and internal dynamics of quadrotor tool operation," *Automatica*, vol. 61, pp. 289–301, 2015.

[16] T. Tomic and S. Haddadin, "Simultaneous estimation of aerodynamic and contact forces in flying robots: Applications to metric wind estimation and collision detection," in *Proc. IEEE International Conference on Robotics and Automation*, 2015, pp. 5290–5296.

[17] K. Hang, X. Lyu, H. Song, J. A. Stork, A. M. Dollar, D. Kragic, and F. Zhang, "Perching and resting—a paradigm for uav maneuvering with modularized landing gears," *Science Robotics*, vol. 4, no. 28, 2019.

[18] K. Zhang, P. Chermprayong, T. Alhinai, R. Siddall, and M. Kovac, "Spidermav: Perching and stabilizing micro aerial vehicles with bio-inspired tensile anchoring systems," in *2017 IEEE/RSJ International Conference on Intelligent Robots and Systems (IROS)*. IEEE, 2017, pp. 6849–6854.

[19] H.-N. Nguyen, R. Siddall, B. Stephens, A. Navarro-Rubio, and M. Kovač, "A passively adaptive microspine grapple for robust, controllable perching," in *2019 2nd IEEE International Conference on Soft Robotics (RoboSoft)*. IEEE, 2019, pp. 80–87.

[20] D. W. Green, J. E. Winandy, and D. E. Kretschmann, "Mechanical properties of wood," *Wood handbook: wood as an engineering material. Madison, WI: USDA Forest Service, Forest Products Laboratory, 1999. General technical report FPL; GTR-113: Pages 4.1-4.45*, vol. 113, 1999.

[21] G.-J. Xiong, J.-J. Chen, J.-H. Wang, and M.-G. Li, "New axisymmetric slip-line theory for metal and its application in indentation problem," *Journal of Engineering Mechanics*, vol. 145, no. 12, p. 04019099, 2019.

[22] P. V.-I. Č.-V. Račko, "The shear strength on the wood/bark border of sessile oak."